Multiple Relaxations of Concentration Fluctuations in Entangled Polymer Solutions

Petr Štěpánek*

Institute of Macromolecular Chemistry, Academy of Sciences of the Czech Republic, Heyrovský Sq. 2, 162 06 Praha 6, Czech Republic

Wyn Brown

Institute of Physical Chemistry, University of Uppsala, Box 532, 751 21 Uppsala 1, Sweden

Received April 2, 1997; Revised Manuscript Received December 22, 1997

ABSTRACT: We have investigated by dynamic light scattering the dynamics of semidilute polymer solutions in a good solvent, specifically polystyrene in benzene. We have shown that, using state-of-the-art instrumentation and data analysis techniques, it is possible to identify in the spectra of relaxation times three very weak slow modes with a combined amplitude of less than 5%, in addition to the dominant cooperative diffusion component (first mode). The results are compared with the predictions of Semenov's theory of dynamics of semidilute solutions in good solvents. The slowest component (fourth mode) was identified as the diffusion of clusters with characteristic size in the range of 100 nm. The third, broad mode corresponds to the reptation process, and finally the second mode is diffusive, with a decay time independent of molecular weight. It is about an order of magnitude slower than the cooperative diffusion and is tentatively assigned to dynamics corresponding to the interentanglement spacing. The three slow relaxation processes only appear for solutions having their concentration or molecular weight above the entanglement limit, c_e or $M_{e,c}$. For $M = 770\,000$ we obtain $c_e \cong 4.0c^*$, with c^* being the usual overlap concentration and for a fixed concentration, of 0.05 g/mL we obtain $M_{e,c} \cong 12M_c^*$, with M_c^* being the overlap molecular weight for this concentration.

Introduction

The dynamics of entangled polymer chains have fascinated physicists for many decades. In particular, de Gennes in his early contributions[1] has laid out the scaling principles of the dynamics of entangled polymer solutions using the reptation concept.

Using the tube model he showed that the relaxation time T_r of a single chain in an entangled solution scales according to $T_r \sim N^3c^{3/2}$, where N is the polymerization index of the polymer, $c > c^*$ is the concentration of polymer in the semidilute solution, and c^* is the overlap concentration for which we accept the usual definition

$$c^* = \frac{M}{(4/3)\pi N_A R^3} \tag{1}$$

where M is the molecular weight of the polymer, N_A Avogadro's number, and R the radius of gyration of the chain. The above result contrasted with the result $T_r \sim N^3c$ found[2] earlier using the Rouse model. The entangled chains form a transient network; T_r is also the lifetime of an entanglement. Two limiting regimes have been considered: at low frequencies ω, $\omega T_r \ll 1$ and the polymer solution displays a liquidlike behavior with a characteristic relaxation rate Γ given by $\Gamma = D_c q^2$, where q is the scattering vector and D_c the cooperative diffusion coefficient. In this hydrodynamic regime, the chains are able to disentangle during the diffusion time $(D_c q^2)^{-1}$. In the high-frequency limit, $\omega T_r \gg 1$ and the solution has a gel-like character with a characteristic relaxational rate denoted as $\Gamma = D_g q^2$ where D_g is the gel diffusion coefficient. The entanglements are frozen on this time scale, and the concentration fluctuations relax as in a permanent gel. Vast experimental work led to advanced understanding of polymer dynamics and of the concept of entanglement which is comprehensively reviewed, e.g., in ref 3. The development of the dynamic light scattering technique[4] made possible direct measurements of the dynamic structure factor.

The dynamic structure factor $S(q,t)$ of a semidilute solution was treated by Brochard and de Gennes[5] and further developed by Adam and Delsanti[6] for the case of solutions under Θ conditions. The latter authors have derived a double-exponential approximation for $S(q,t)$.

$$S(q,t) = A_1 \exp(-\Gamma_1 t) + A_2 \exp(-\Gamma_2 t) \tag{2}$$

Under the generally fulfilled experimental condition $q < (T_r D_g)^{-1/2}$, they obtained

$$\Gamma_1 = D_g q^2 = \frac{\mu}{c}(E_{os} + E_g)q^2 \tag{3}$$

$$\Gamma_2 = \frac{D_c}{D_g T_r} = \frac{E_{os}}{(E_{os} + E_g)T_r} \tag{4}$$

$$\frac{A_2}{A_1} = \frac{E_g}{E_{os}} \tag{5}$$

where E_g is the shear elastic modulus of the transient gel, E_{os} its osmotic modulus, and μ the effective monomer mobility.[6] Thus in this approach, the fluctuation of concentration induces a concentration gradient and an elastic stress. At times $t < T_r$, at which the solution behaves as a permanent gel, the concentration fluctuation relaxes with a decay time $\tau_1 = \Gamma_1^{-1}$. At times $t > T_r$ the chains can disentangle and the elastic stress relaxes with a decay time $\tau_2 = \Gamma_2^{-1}$.

Equations 3−5 have been derived for the case of a Θ solvent where E_{os} and E_g are of the same order of

S0024-9297(97)00458-0 CCC: $15.00
Published on Web 02/28/1998

magnitude, but using appropriate values of E_{os} and E_g, they also describe the good-solvent system considered in this contribution. Thus, for example,[6] under Θ conditions and at a concentration of $c = 0.05$ g/cm^3, we have[6] $E_{g,\Theta} = 3820$ dyn/cm^2 and $E_{os,\Theta} = 3750$ dyn/cm^2; thus, $E_{g,\Theta}/E_{os,\Theta} \cong 1$; according to eq 5, we expect that the two components of $S(q,t)$ will have approximately the same amplitude. In a good-solvent system, on the other hand, E_g decreases slightly but E_{os} increases strongly; typically,[6] $E_g = 0.9E_{g,\Theta}$ but $E_{os} = 32E_{os,\Theta}$. Then $A_2/A_1 \cong 0.04$ and it has been concluded in ref 6 and also shown experimentally by several authors that the longest decay time is, in principle, undetectable and the dynamic structure factor of a semidilute solution in a good solvent can be considered as single-exponential.

We note here that Doi and Onuki[7] also used a starting point similar to that of Brochard and de Gennes and presented a general phenomenological theory yielding a dynamic structure factor with a form similar to that of eq 2. Their result includes a characteristic length for the viscoelastic process which describes a dynamic coupling between the concentration fluctuations and the viscoelasticity resulting in the slow structural relaxation. As the solvent quality is increased, the diffusive mode becomes dominant. Eventually, in a good solvent, $E_{os} \gg E_g$ so that $A_2 \ll A_1$.

No systematic search has been reported for the possible presence of the longest disentanglement mode in polymer solutions in a good solvent. However, in 1988 we examined[8] solutions of polystyrene in toluene, and by subtracting the main diffusive gel mode, we found evidence for the presence of additional, slowly decaying modes with very small amplitudes which had previously been undetected. At that time, neither the state of the art of the instrumentation and data analysis nor the available theoretical background permitted a more quantitative assessment of this finding.

In 1990, Semenov[9] considered both the elastic deformation of the entanglement network and the entanglement dynamics of the individual chains for good-solvent systems and, using a mean-field approach, calculated the concentration time correlation function. He found that relaxation of concentration fluctuations in a semidilute polymer solution proceeds in three stages with considerably different times: the cooperative stage with relaxation time τ_c, the Rouse stage with relaxation time τ_R, and the reptation stage with relaxation time τ_{rp}. Thus, the earlier experiments[8] would appear to lend support to this theory.

The purpose of this investigation is to present careful and detailed measurements of dynamic light scattering on semidilute solutions of polystyrene in a good solvent, benzene, which is an athermal system, and to compare the properties of the observed slow modes to the predictions of Semenov's theory.

Theory

First, we briefly review the essential conclusions of Semenov's theory,[9] relevant to this work. Although we have used a wide range of polymer molecular weights M_w, semidilute solutions only exist, at the selected concentration of 5%, for relatively large molecular weights, $M_w = 10^5-10^7$ (see below); given the wavelengths of visible light, the experiments are thus conducted at $qR \gtrsim 1$, where q is the scattering vector. In this region, the dynamic structure factor has the form

$$S(q,t) = v[A_c\, g_c(t) + A_R g_R(t) + A_{rp} g_{rp}(t)] \qquad (6)$$

where v is a parameter describing volume interactions. Equation 6 shows that $S(q,t)$ relaxes in three stages: the usual cooperative stage, the Rouse-like stage, and the reptational stage.

Using the notation of ref 9, we take $\delta = E_g/E_{os}$ and the cooperative stage is described by

$$A_c = 1/(1 + \delta) \qquad (7)$$

$$g_c(t) = \exp[-(1 + \delta)D_c q^2 t] \qquad (8)$$

where D_c is the cooperative diffusion coefficient. As we have noted in the Introduction, δ is very small, typically $\delta \sim 0.04$; thus, A_c is close to unity and the amplitudes of the other two stages are small.

At longer times, the relaxation proceeds by the Rouse stage. Along the tube axis, some parts of the macromolecules are stretched and some are compressed. Such tension along the polymer chain tends to redistribute the links, with a Rouse relaxation time τ_R and a small amplitude $A_R \simeq \delta/6$. This process leads to a slight decrease of the elastic modulus from E_g to $\bar{E}_g$, with $\bar{E}_g \cong 0.8E_g$ for $qR > 1$. It is this new elastic modulus $\bar{E}_g$ which governs the last reptational stage of relaxation. Its amplitude is

$$A_{rp} = \bar{E}_g/(\bar{E}_g + E_{os}) \qquad (9)$$

and the process is not single-exponential; it is characterized by a spectrum of relaxation times between τ_{rp} and the longest relaxation time τ^*.

Depending on the value of the scattering vector q and of the polymerization index N, the relaxation times of the three stages have different dependences on the variables q and N, as summarized in Figure 1, based on Semenov's theory. Here, the radius of gyration of the polymer is

$$R = aN^{1/2} \qquad (10)$$

and in the theoretical treatment this relation is considered valid also for a semidilute solution, provided that a is treated as an effective renormalized size depending on concentration.

In this work, we have investigated by dynamic light scattering the dynamics of such semidilute polymer solutions using polystyrene standards covering a wide range of molecular weights ($M = 2 \times 10^3-20 \times 10^6$) dissolved in benzene. We have selected a concentration of 5%, which is large enough to reach substantial entanglement for higher molecular weights but is low enough to be able to observe dynamics within the accessible time window of dynamic light scattering.

Figure 2 shows the various crossovers indicated in Figure 1 as a function of the polymerization index N and inverse scattering vector q^{-1} calculated for polystyrene, using $N = M_w/104$. Since for molecular weights above 4×10^5 the boundary $qR = 1$ lies within the range of accessible scattering vectors q, we have exercised great care in correctly determining the value of the radius of gyration and thus of the parameter a in eq 10. Indeed, as the concentration of a polymer solution is increased, the radius of gyration of a polymer chain decreases and does so even in the semidilute range (to reach eventually the unperturbed dimension in bulk). While scaling theory predicts[10] for the concentration

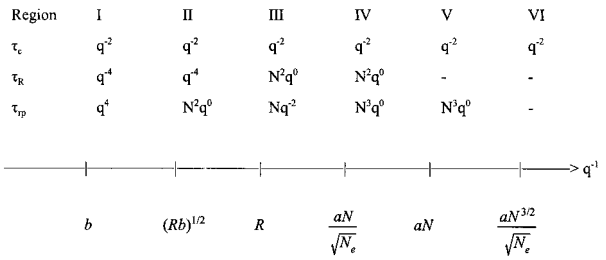

Figure 1. Dependence on N and q of the three relaxation times τ_c, τ_R, and τ_{rp} as a function of the length scale q^{-1}. Here, R is the radius of gyration of the polymer chain, a is defined by eq 10, and $b = aN_e^{0.5}$ is the tube diameter. Note the anomalous q^4 dependence of τ_{rp} in region I.

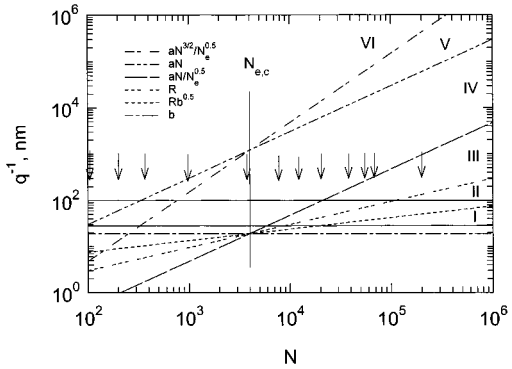

Figure 2. Representation of crossovers between various regions of Semenov's theory, as they appear in Figure 1, in terms of the polymerization index N and scattering vector q. The legend to the lines is arranged in the order in which the lines intersect the right side of the figure. The various lines have been calculated for polystyrene, used in this work, with monomer molecular weight $m = 104$ and entanglement polymerization index $N_{e,c}$ corresponding to a concentration of 5%. The two horizontal lines represent the range of scattering vectors available with scattering angles between 30° and 140°.

Table 1. Characteristics of the Polystyrene Standards Used

$M_w \times 10^3$	M_w/M_n	c^*, g/mL	R_g (c = 0.05), nm	producer
2	1.3	0.19	1.6	Polyscience
4	1.04	0.14	2.2	Polyscience
10	1.2	0.088	3.5	Polyscience
20	1.06	0.062	5	Polyscience
37	1.06	0.046	6.8	Pressure Chemicals
98	1.1	0.028	11.1	Pressure Chemicals
390	1.1	0.014	22.1	Pressure Chemicals
770	1.01	0.01	31.1	Toyo Soda
1260	1.05	0.0079	39.8	Toyo Soda
2000	1.2	0.0063	50.2	Pressure Chemicals
3840	1.04	0.0045	69.6	Toyo Soda
5480	1.15	0.0038	83.1	Toyo Soda
6770	1.14	0.0034	92.3	Toyo Soda
20000	1.35[a]	0.002	158.8	Toyo Soda

[a] Reference 14.

dependence of R_g in semidilute solution the scaling behavior $R_g^2 \sim c^{-0.25}$, experiments[10,11] are more in favor of a smaller exponent, $R_g \sim c^{-0.20}$. From values of R_g for polystyrene measured in ref 11 for various concentrations and molecular weights, we have derived actual values of R_g at the concentration of 5% and the molecular weights used in this work. These values of R_g are included in Table 1, and they were used in plotting the lines in Figure 1. They also lead to an approximate value $a = 0.0355$ nm for the parameter a in eq 10. The two horizontal lines in Figure 1 delimit the available range of scattering vectors, whereas the vertical line marked $N_{e,c} \cong 4000$ locates the entanglement molecular weight for the concentration $c = 5\%$, obtained using the relation[12]

$$N_{e,c} = N_e/c \tag{11}$$

where N_e is the entanglement polymerization index in the bulk, which is taken[13] as $N_e \cong 200$.

The vertical bars indicate the individual polymer samples that have been used. It is clear that the experimentally accessible region of entangled solutions ($N > N_{e,c}$) is located almost entirely in the regions II and III of Figure 1 where Semenov's theory predicts

$$\text{region II} \quad \tau_c \sim q^{-2}N^0 \quad \tau_R \sim q^{-4}N^0 \quad \tau_{rp} \sim q^0N^2 \tag{12}$$

$$\text{region III} \quad \tau_c \sim q^{-2}N^0 \quad \tau_R \sim q^0N^2 \quad \tau_{rp} \sim q^{-2}N \tag{13}$$

Clearly, the various lines drawn in Figure 2 do not represent sharp boundaries but smooth crossovers from one type of behavior to another. The main purpose of this contribution is to compare the properties of the various decay modes observed in good-solvent semidilute solutions with the predictions of Semenov's theory.

Experimental Section

The polymers used are the atactic polystyrene standards listed in Table 1 purchased from the indicated suppliers; the polydispersity index of the highest molecular weight was determined in ref 14. The solvent, benzene (Fluka), and cosolvent, cyclopentane (Fluka), were dried over calcium hydride and freshly distilled before use. Since semidilute solutions of high-molecular-weight polymers are too viscous to be filtered directly, the samples were prepared in a two-step procedure. In the first step, polystyrene solutions in cyclopentane with a concentration $c < 3c^*$ were prepared and centrifuged for 1 h at 15 000 rpm. Using dedusted plastic syringes, the upper two-thirds of the solution were transferred into dedusted light scattering cells, and cyclopentane was evaporated until a constant weight of the cells was reached. Then the appropriate amount of benzene, filtered through a 0.2-μm Millipore filter, was added, and the cells were flame-sealed. The final concentrations were determined by weighing. The solutions were left to homogenize at room temperature for an extended period of time, which, due to some technical and organizational issues, turned out to be 12 months.

The dynamic light scattering apparatus consists of an ALV5000/E logarithmic correlator, of a goniometer with an index-matching vat filled with decalin. The light source was a Coherent Innova 304 Ar laser operated at 488 nm in the power track mode which ensured the necessary laser stability required for these kinds of measurements. The scattered light was detected in a VV geometry with a ITT FW 130 photomultiplier coupled to a single-mode optical fiber.

As the expected amplitudes of the slow modes are extremely small (on the order of a few percent) in a good-solvent semidilute solution, long accumulation times (typically 1 h) were needed to reach good statistics in the slow part of the correlation function. Despite all the care exercised during the sample preparation and filtration of the index-matching liquid, some dust particles are unavoidably present in the solutions and in the index-matching liquid. Their passage through the scattering volume, in its vicinity, or through the incident beam (a few times per hour) is visually observable through a microscope, and their effect is usually dropped into the "dust" baseline term of the correlation function. In the present experiments, however, it has a devastating effect on the extraction of low-amplitude slow contributions from the data. Therefore, when necessary, a number of shorter runs of

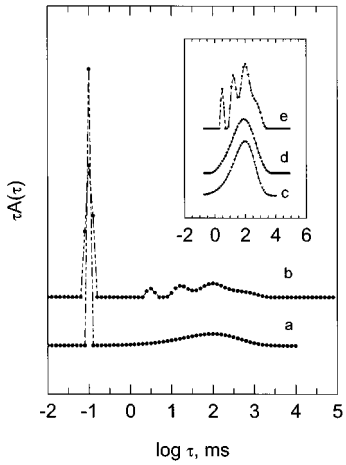

Figure 3. Simulated distribution function, as described in the text (curve a) together with inverse Laplace transformation analysis before subtraction of the narrow, fast component (curve b). The inset shows the slow part of the distribution function as simulated (curve d), as recovered after subtraction (curve c), and before subtraction (curve e).

durations of 1−5 min were accumulated, correlation functions influenced by passage of dust were excluded, and the remaining correlation functions were summed before final analysis. Depending on the quality of the sample, up to 20% of the measurements was discarded in this way.

The correlation functions were analyzed using an inverse Laplace transformation program Repes,[15] which, from the measured intensity correlation function $g^2(t)$, yields the distribution of relaxation times $A(\tau)$ according to

$$g^2(t) - 1 = \alpha[\int A(\tau) \exp(-t/\tau)\, d(\tau)]^2 \qquad (14)$$

where α is an instrumental parameter. This program differs from the widely used program[16] CONTIN in that it fits directly the measured intensity correlation function $g^2(t)$. Since the measurements cover a large number of decades in relaxation time, the resulting distributions have to be presented in the equal-area presentation, $\tau A(\tau)$ vs log τ.

The cooperative diffusion process is a very strong component in these measurements and is represented by a very narrow peak with an amplitude on the order of 95%. It has been shown previously[17,18] that the presence of such a component induces, via the so-called δ-effect, artifacts in the distribution of relaxation times obtained from a Laplace inversion. Therefore, after a first analysis yielding the relaxation time and amplitude of the cooperative diffusion process, we have systematically subtracted this component from the correlation functions, according to the procedure described in refs 19 and 20. The new correlation function was then reanalyzed to yield the relaxation times and amplitudes of the slow modes. Figure 3 illustrates this procedure on simulated data. We have generated a distribution function of relaxation times (curve a in Figure 3) which consists of two contributions: one is a narrow Gaussian function centered at log $\tau = -1$; the other is a broad generalized exponential function centered at log $\tau = 2$. Then we have numerically integrated eq 14 to obtain a synthetic correlation function, adding a 1% random noise to the data. This was then analyzed using the inverse Laplace transformation program, and the distribution of relaxation times labeled b was obtained. While the dominant narrow peak (simulating the cooperative diffusion mode) is correctly recovered, we observe artifactual breaking into several peaks of the originally smooth broad contribution at long delay times. The dominant peak was then subtracted from the correlation function and the remainder re-analyzed. The resulting distribution (curve c) now represents only the slow broad contribution, which is compared in the inset of Figure 3 in an enlarged form to the original simulated distribution (curve d) as well as to the distribution obtained in the first analysis (curve e). The subtraction procedure has clearly removed the artifactual peaks and produced a distribution of relaxation times very close to the simulated one.

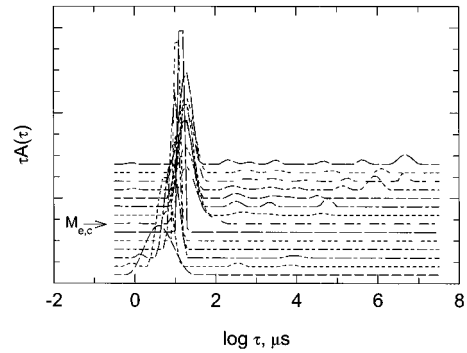

Figure 4. Distribution function of relaxation times in equal area representation, $\tau A(\tau)$ vs log τ obtained on solutions of polystyrene standards in benzene with concentration $c = 0.05$ g/mL. The molecular weight increases from bottom to top in the order in which the polymer samples are listed in Table 1.

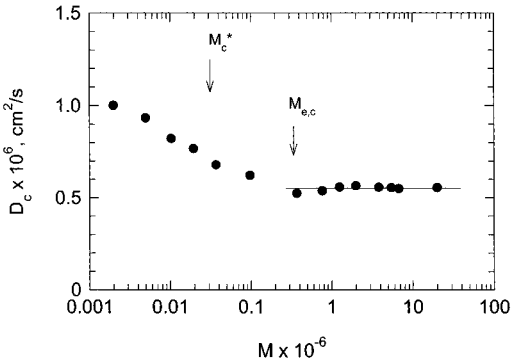

Figure 5. Dependence of the cooperative diffusion coefficient D_c on molecular weight M, for solutions of polystyrene in benzene at a concentration of 0.05 g/mL. The arrows indicate values of M_c* determined from eq 1 and of $M_{e,c}$ determined from eq 11, always for $c = 0.05$ g/mL.

Results and Discussion

A. Effect of Molecular Weight at Fixed Concentration. Figure 4 shows the distributions of decay times obtained for various molecular weights, always on a solution of concentration 5%. The dominant peak located at short times corresponds, of course, to the cooperative diffusion process which has been extensively studied in the existing literature (e.g., ref 21). The corresponding diffusion coefficient D_c is plotted as a function of molecular weight in Figure 5. At the fixed concentration of 5%, D_c reaches a molecular-weight-independent value in the vicinity of $M = 400\,000$, which, as seen on Figure 5, is much closer to the entanglement molecular weight $M_{e,c}$ than to the overlap molecular weight M_c*. $M_{e,c}$ was calculated using the entanglement molecular weight of polystyrene in bulk,[12] $M_e = 17\,300$, and eq 11; we obtain $M_{e,c} = 350\,000$.

It is interesting to compare $M_{e,c}$ with the "overlap" molecular weight M_c* corresponding to $c = 5\%$, as calculated from the usually accepted expression (eq 1) in which we replace R_g by eq 10. For $c = 5\%$, we obtain $M_c^* = 31\,000$ so that the entanglement molecular weight $M_{e,c}$ differs from the overlap molecular weight M_c* by a factor of $M_{e,c}/M_c^* \cong 12$. The value of this ratio is, however, specific to the particular concentration used. In fact, combining eqs 1 and 11, we obtain for the ratio of entanglement molecular weight and crossover mo-

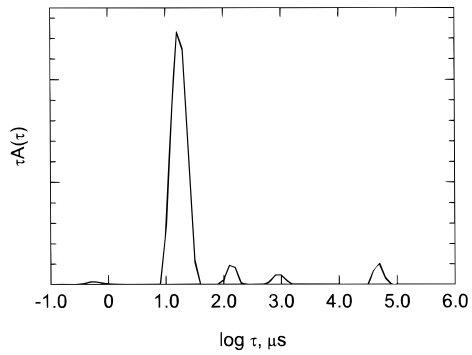

Figure 6. Distribution of relaxation times obtained on a solution of polystyrene ($M_w = 1.26 \times 10^6$) in benzene with concentration 0.05 g/mL, at a scattering angle of 90°.

lecular weight $M_{e,c}/M_c^* \cong 230c$ so that this quantity depends linearly on concentration.

We should note also that cooperative diffusion is a physical process related to the screening length (i.e., on the binary contacts or the blob size) and is not connected to entanglements. We shall discuss below the relation between blobs and entanglements. The data on Figure 5 thus simply mean that the cooperative diffusion coefficient has not reached its asymptotic scaling behavior $D_c \sim M^0$ until M is substantially larger than M_c^*. Such a finding is common when scaling properties of various quantities are examined, and it has been discussed in the literature previously; see, e.g., refs 21 and 22.

Applying the Stokes−Einstein equation to the cooperative diffusion coefficient D_c, $D_c = kT/6\pi\eta_0\xi$, where k is the Boltzmann constant, T the absolute temperature, and η_0 the solvent viscosity, we obtain the corresponding correlation length of fluctuations in concentration ξ, i.e., the "blob" size or average distance between binary contacts of polymer chains in the semidilute solutions. For the plateau value of D_c for solutions with $c = 5\%$ in Figure 5, $D_c = 0.5 \times 10^{-6}$ cm^2/s, we get $\xi = 7.2$ nm.

For molecular weights larger than $M_{e,c}$, we observe in Figure 4 several very weak components at relaxation times larger than that of D_c. Figure 6 shows a particular distribution of decay times for the molecular weight $M = 1.26 \times 10^6$ which exhibits three slow relaxation processes of amplitude 1−5% each. Using the subtraction technique described above to eliminate the δ-effect of the fast cooperative diffusion peak, we could establish that for $M > M_{e,c}$ the slow part of the distribution of relaxation times always consists of three low-amplitude components. Their properties are discussed below.

Figure 7 summarizes the molecular weight dependence of the various relaxation times extracted from the correlation functions, including that corresponding to the cooperative diffusion. The full line represents the longest viscoelastic relaxation time T_R obtained rheologically[23] on the same system, polystyrene/benzene. For all molecular weights investigated the slowest component is slower that T_R and, as shown in Figure 8a for the sample with $M_w = 1.26 \times 10^6$, it is diffusive (since $\Gamma \sim q^2$). Interpolating viscosity data for this system given in ref 23, we obtain for the solution used in Figure 8 a viscosity $\eta = 1.13$ Pa. We can now estimate the hydrodynamic size of the diffusing object using the Stokes−Einstein equation, $R_h = kT/6\pi\eta D$, where R_h is the hydrodynamic radius of the object, k is the Boltzmann constant, T is the absolute temperature, and D the diffusion coefficient of that object. We obtain a

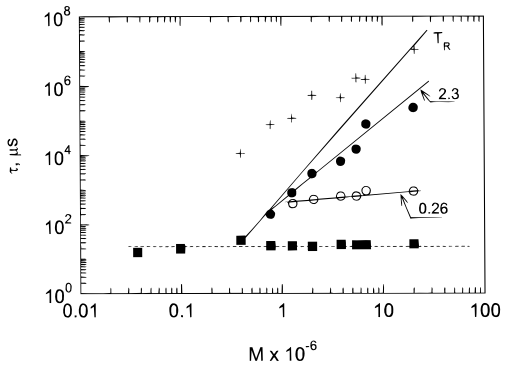

Figure 7. Dependence on molecular weight of the various relaxation times of polystyrene solutions in benzene at a concentration of 0.05 g/mL: (+) cluster mode, (■) cooperative diffusion mode, (○) mode I, (●) mode II. The full line marked T_R represents the longest viscoelastic relaxation time and is calculated on the basis of data given in ref 23.

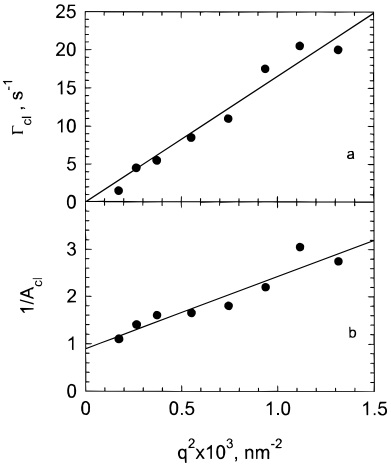

Figure 8. (a) Dependence on q^2 of the decay rate Γ_{cl} of the cluster mode for a solution of polystyrene ($M_w = 1.26 \times 10^6$) in benzene, concentration 0.05 g/mL. (b) Dependence on q^2 of the inverse amplitude of the cluster mode, A_{cl}, for the same sample.

hydrodynamic size corresponding to the slowest, diffusive component of $R_h = 115$ nm. We are thus led to the conclusion that this component corresponds to clusters, often observed in dense systems such as melts of polymers[24] or block copolymers,[25,26] concentrated solutions,[27] or even low-molecular-weight glass-forming liquids.[28] This conclusion is supported by Figure 8b, which shows the dependence of the inverse relative intensity of the cluster component on q^2. The observed linear dependence has been fitted with the Ornstein−Zernicke expression, $I(q) = I(0)/(1 + q^2\xi^2)$, yielding a static correlation length $\xi = 44$ nm. The agreement of both estimations of the size of the cluster is reasonable given the fact that one method is static and the other dynamic and that there is some scatter in the experimental data in Figure 8. The present findings are particular in that the cluster component is observed (although with a very small amplitude) in a moderately concentrated system, $c = 5\%$. As is apparent in Figure 7 (and also Figure 16), this cluster component is, however, observed only in solutions exceeding the entanglement limit, expressed in terms of either M_e or c_e (the concentration dependences of relaxation times involving c_e are described below). Our findings are corroborated by a recent observation of Heckmeier et al.[29] of clusters in the 100-nm size range by dynamic

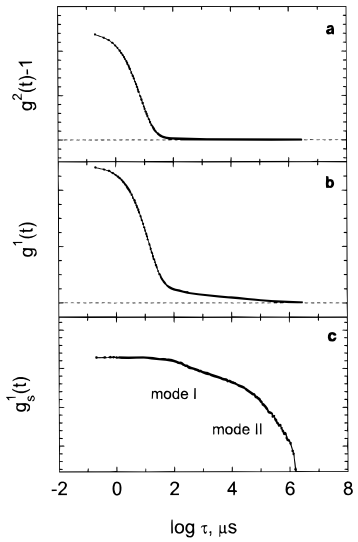

Figure 9. Correlation functions obtained on a solution of polystyrene ($M_w = 6.77 \times 10^6$) in benzene at a concentration 0.05 g/mL: (a) intensity correlation function $g^2(t) - 1$; (b) field correlation function $g^1(t)$; (c) field correlation function $g_s^1(t)$ after subtraction of the cooperative and cluster diffusion components.

light scattering in moderately concentrated polystyrene/toluene solutions.

The remainder of this paper deals with the analysis and identification of the remaining two relaxation processes observed in the correlation function obtained on semidilute solutions. Of the 14 different molecular weights used in this work, only the 7 highest reach the entanglement regime at the concentration of 0.05 g/mL. A typical correlation function obtained on a sample with $M_w = 6.77 \times 10^6$ is shown in greater detail in Figure 9, which emphasizes the weakness of the slow modes. Indeed, Figure 9a shows the intensity correlation function as measured; to the naked eye it has the appearance of a single-exponential function. Figure 9b shows the corresponding field correlation function in which the slow relaxations are apparent. Figure 9c displays, with a logarithmic vertical axis, the field correlation function $g_s^1(t)$ from which the cooperative and cluster diffusion components were subtracted. Clearly, two modes are observed in Figure 9c, labeled mode I and mode II. We have found that in all the cases examined mode II was a broad component while mode I remained quite narrow. Accordingly, correlation functions $g_s^1(t)$ were fitted with a double Williams−Watt function

$$g_s^1(t) = A_1 \exp[-(t/\tau_I)^{\beta_I}] + A_{II} \exp[-(t/\tau_{II})^{\beta_{II}}] + B \quad (15)$$

where the exponents β_i describe the width of the relaxation process. As will be shown below, typical values of the exponents are $\beta_{II} \cong 0.5$ for mode II and $\beta_I \cong 1$ (i.e., single-exponential) for mode I.

As is apparent in Figure 2, for molecular weights above $M_{e,c}$ the available range of scattering vectors q covers essentially regions II and III of Semenov's theory. The majority of feasible experiments lies in region II, which we discuss first. Figure 10 shows the angular dependence of the decay rate of mode II for the molecular weight $M_w = 6.77 \times 10^6$ which offers the largest angular range in region II (the largest molecular weight $M_w = 20 \times 10^6$ produces relaxation times so slow that they are only determined with a larger error). Clearly, the decay rate of mode II is angle-independent. The

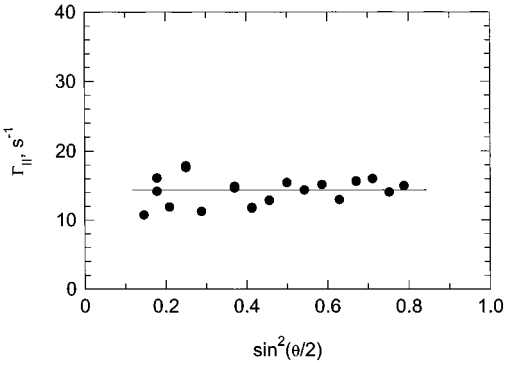

Figure 10. Dependence on $\sin^2(\theta/2)$ of the decay rate Γ_{II} of mode II for the solution of polystyrene with $M_w = 6.77 \times 10^6$.

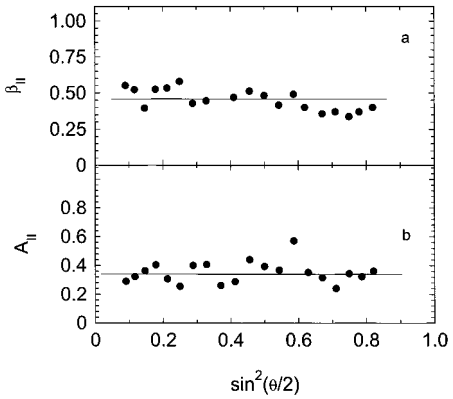

Figure 11. Dependence on $\sin^2(\theta/2)$ of the width of mode II, as described by the parameter β_{II}, and of its fractional amplitude A_{II} (relative to that of mode I + mode II), for the solution of polystyrene with $M_w = 6.77 \times 10^6$.

width of the distribution of relaxation times of this mode, as described by the parameter β_{II}, has the value of approximately 0.4 for all the angles, as shown in Figure 11a, meaning that the whole distribution of relaxations constituting this mode is angle-independent. Figure 11b shows that the fractional amplitude of this mode (relative to that of mode I + mode II) is also angle-independent.

The molecular weight dependence of the decay time of this mode is shown in Figure 7, summarizing results from measurements at the angle 100°. The experimental data for this mode can be fitted with a straight line, with a slope 2.3 ± 0.4 representing the exponent in the dependence of Γ on M. The relatively large uncertainty of the exponent is due to the fact that only 7 data points are available in a range of molecular weight covering only 1.4 decades. Nevertheless, this mode can be identified with the reptation mode in region II of Figure 2 as described by the last term in eq 12: $\tau_{rp} \sim q^0 N^2$.

The final stage of relaxation due to reptation consists of a relatively broad distribution of relaxation times, characterized experimentally by the exponent β_{II}. Theoretically, the average reptation time τ_{rp} is approximated as[9]

$$\tau_{rp} = 2\tau^*/\Delta$$

In eq 13, τ^* is the longest relaxation time for which $\tau^* \sim N^3$ holds[9] and $\Delta = cvN$, where v is a parameter characterizing volume interactions between polymer segments such as in eq 6. Δ depends on N and on the osmotic and elastic moduli of the polymer solutions. It cannot be quantitatively well-assessed but is large,[9]

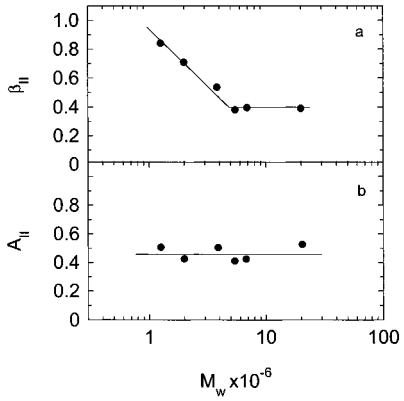

Figure 12. Dependence on molecular weight M_w of (a) the width parameter β_{II} and (b) fractional amplitude A_{II} (relative to that of mode I + mode II) for mode II.

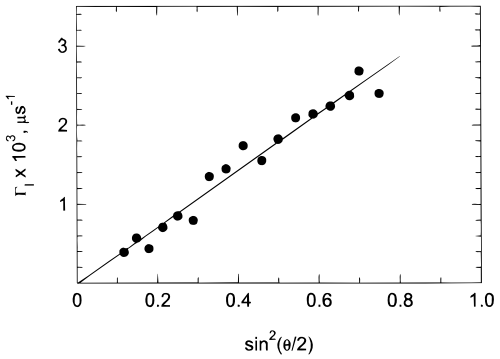

Figure 13. Dependence of the decay rate Γ_I of mode I on $\sin^2(\theta/2)$ for the solution of polystyrene with $M_w = 6.77 \times 10^6$.

which explains that τ_{rp} is rather short compared to τ^* (see Figure 7). The width of the distribution of relaxation times for mode II increases with increasing molecular weight, as quantified by the decreasing parameter β_{II} shown in Figure 12a. For the larger molecular weights β_{II} reaches a constant of about $\beta_{II} = 0.37$. The decrease of β_{II} may be due either to an overlap of the short-time tail of the distribution with the two faster relaxation modes or to a narrowing of the distribution as molecular weight is decreased. We prefer the second explanation since the fractional amplitude of the slow mode, as shown in Figure 12b, is constant as a function of molecular weight, which excludes the possibility that part of the broad relaxation distribution of mode II was included in mode I.

The faster mode is always almost single-exponential (β_I very close to 1) and is diffusive in character, as is demonstrated by the linear dependence of its decay rate, Γ_I, on $\sin^2(\theta/2)$ shown in Figure 13. As a function of molecular weight, the decay rate of mode I is almost constant, as can be seen in Figure 7. Given the same experimental uncertainty in the data as for mode II, we are not sure whether the small slope of 0.26 ± 0.20 in Figure 7 yielded by a linear fit has any real significance. We rather prefer to describe this mode as being diffusive and independent of molecular weight. This is in contrast with Semenov's theory which predicts that there exists a Rouse mode in the dynamic structure factor whose relaxation time is localized between that for cooperative diffusion and that for reptation; in region II of Figure 2 it should have the properties $\tau_R \sim q^{-4}N^0$; its amplitude, however, is predicted[9] to be almost an order of magnitude smaller than that of the reptation mode, already very weak, so that it may not be detectable in the presence of the other modes. The failure to observe Rouse dynamics by dynamic light scattering was reported earlier experimentally by Martin[30] and by Wiltzius[31] and discussed theoretically by Oono.[32]

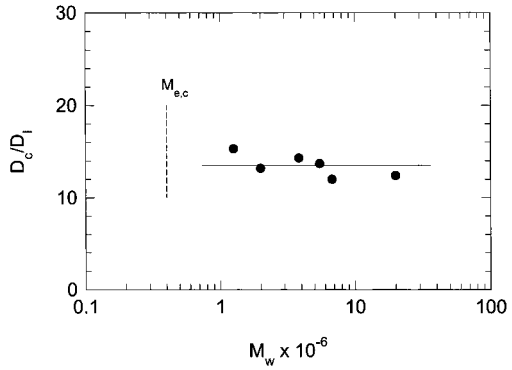

Figure 14. Dependence on molecular weight of the ratio of the cooperative diffusion coefficient D_c to the diffusion coefficient corresponding to mode I, D_I.

In fact, mode I behaves in the same way as the cooperative diffusion except that it corresponds to a correlation length which is about an order of magnitude larger than ξ. Figure 14 shows the ratio of diffusion coefficients D_c and D_I for the cooperative mode and mode I, which is at the same time the ratio of the characteristic length associated with mode I, ξ_I, to the correlation length ξ. Within experimental uncertainty, this ratio is constant, with an average value $D_c/D_I = \xi_I/\xi = 13.5$. We now show that ξ_I has the same length as the distance between entanglements, ξ_e. Indeed, Raspaud et al.[33] have demonstrated, on the basis of measured values of osmotic and shear elastic moduli, that the number of blobs per entanglement n_e is independent of concentration, and for semidilute solutions of polystyrene in benzene, they have found the average value $n_e = 185 \pm 40$. Since a chain of blobs behaves as a Gaussian chain, we may write $\xi_e = \xi\sqrt{n_e}$. This yields $\xi_e/\xi = 13.6 \pm 1.5$, which is almost the same as the ratio obtained in Figure 14. So we conclude that $\xi_I = \xi_e$ and that two characteristic lengths ξ and ξ_e determine the properties of a semidilute good-solvent solution, in agreement with recent theoretical work by Fuchs and Schweizer.[34] The fact that the number of blobs per entanglement n_e (and thus ξ_e/ξ) is a nonuniversal quantity characteristic of a given polymer leads to a failure of scaling laws when dynamic measurements for different polymers are compared.[33]

For low molecular weights, but still above $M_{e,c}$ and for small angles, a part of region III of the diagram in Figure 2 is accessible. Figure 15 displays the angular dependence of the decay rates of modes I and II for a 5% solution of polystyrene with $M_w = 1.26 \times 10^6$. The decay rate of mode II (Figure 15a) is proportional to q^2 at small angles, with a deviation toward a q-independent behavior for angles $\theta > 110°$. For this angle we have $qR = 1.15$. For smaller angles the data belong to region III with $qR < 1$ where Semenov's theory predicts $\Gamma \sim q^2$ as indeed we observe; for larger angles there is a gradual crossover into region II with $qR > 1$, which was more closely examined above. For mode I the expected behavior $\Gamma \sim q^0$ changing into $\Gamma \sim q^4$ is again not observed (see Figure 15b), and instead we find that mode I is diffusive, $\Gamma \sim q^2$ as in region II. For light scattering wave vectors q region III is so small that we cannot examine the molecular weight dependence of the individual modes.

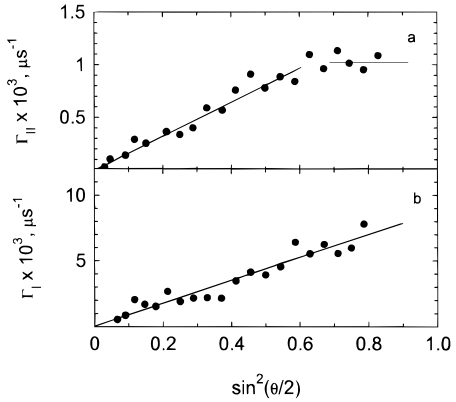

Figure 15. Dependence of the decay rates Γ_{II} and Γ_I on $\sin^2(\theta/2)$ for the solution with $M_w = 1.26 \times 10^6$.

B. Effect of Concentration at Fixed Molecular Weight. The concentration dependence of various relaxation times has been investigated for the molecular weight $M_w = 770\,000$ and is displayed in Figure 16. A clear change of behavior is observed in the vicinity of $c = 2\%$ which corresponds to the entanglement concentration c_e. Below c_e, the dominant decay corresponds to the translational diffusion of polymer coils, whereas the faster, weak contribution corresponds to a combination of the angle-independent internal mode of the polymer chain and its diffusive translation mode. The dependence of the decay rate of this mode on q^2 has a nonzero intercept at $q = 0$ from which the relaxation time of the internal mode, $\tau_1 = 80\,\mu$s, can be determined. A more complete study of the internal mode is not a subject of this work, but this value is in agreement with values determined previously[35] on similar systems as well as with theoretical predictions[35] yielding $\tau_1 = 60\,\mu$s.

Above c_e, the dominant mode is the cooperative diffusion mode which is the fastest in Figure 16. Simultaneously, the slower modes appear. Using eq 11, we find that the entanglement concentration for polystyrene with $M_w = 770\,000$ is $c_e = 2.2\%$, in good agreement with the experimentally observed value. Compared with $c^* = 0.54\%$ as determined from eq 1, we find that $c_e/c^* \cong 4.0$. This finding is similar to that discussed above for $M_{e,c}/M_c^*$. Using again eqs 1 and 11 we obtain $c_e/c^* \cong 2000M^{-0.5}$ so that this ratio decreases with increasing molecular weight.

The slowest component in Figure 16 is again slower that the longest viscoelastic relaxation time and therefore assigned to cluster diffusion. The experimental points for this mode are substantially scattered in line with its poorly defined character. We also see that this cluster mode is not present in unentangled solutions, at $c < c_e$.

The concentration dependence of the decay time for the cooperative diffusion mode for $c > c_e$ in Figure 16 can be fitted with a straight line, yielding a concentration exponent of -0.61. This value is smaller than the theoretical value[36] -0.75 but in agreement with previously published results on many different systems.[21] The exponents for the concentration dependences of the relaxation times of mode I (related to the entanglement spacing) and mode II (reptation) are difficult to determine, since the semidilute region covers less than a decade in concentration units. We did not want to use solutions with concentration above $c = 20\%$ since it would be questionable whether such solutions can still be considered as semidilute. A much larger molecular weight would be needed to extend the semidilute range on the low-concentration side, but we did not have enough high-molecular-weight polymer to prepare a large number of highly concentrated samples. Such experiments are planned for the near future. In any case, Semenov's theory does not make explicit predictions for the concentration dependence of relaxation times, since concentration effects are included in the renormalized parameter a in eq 10. On the other hand, for mode I we observe, in Figure 16, a trend in concentration behavior similar to that of the cooperative diffusion. Since Figure 16 is logarithmic, this means that approximately we have $\xi_e \sim \xi$, in agreement with the finding by Raspaud et al.[33] that the number of blobs per entanglement does not depend on concentration.

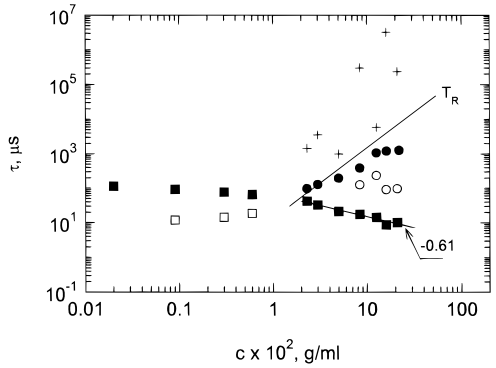

Figure 16. Concentration dependence of relaxation times of the various modes for solutions of polystyrene with $M_w = 770\,000$ in benzene: (+) cluster mode, (○) mode I, (●) mode II, (■) cooperative diffusion mode, (□) internal mode. The full line marked T_R represents the longest viscoelastic relaxation time calculated from data in ref 23.

Conclusion

We have shown in this contribution that, with careful experiments and high-quality solutions, it is possible to detect in semidilute entangled solutions in good solvents three low-amplitude slow modes, in addition to the usual cooperative diffusion mode. The slowest mode is attributed to the diffusion of large clusters. Of the other two modes, the slower one is shown to be the reptation mode predicted by Semenov's theory. The faster one is not the Rouse mode predicted by this theory but is diffusive, with a decay rate proportional to that of the cooperative diffusion mode. It is attributed to dynamics corresponding to the length scale of interentanglement spacings. We have also shown that the various slow modes exist only for concentrations or molecular weights such that the polymer chains are truly entangled (not only overlapping). Work is in progress to extend the present results to semidilute solutions in marginal and Θ solvents.

Acknowledgment. We thank Professor Semenov for valuable comments to the present work. We gratefully acknowledge support by the Grant Agency of the Academy of Sciences of the Czech Republic under Grant A4050604 and by the Swedish National Science Research Council (NFR). P.S. thanks the University of Uppsala for travel support.

References and Notes

(1) de Gennes, P. G. *Macromolecules* **1976**, *9*, 587, 594.
(2) Rouse, P. E. *J. Chem. Phys.* **1953**, *16*, 565.

(3) Graessley, W. *Adv. Polym. Sci.* **1974**, *16*, 1.
(4) Berne, B. J.; Pecora, R. *Dynamic Light Scattering*; John Wiley & Sons: New York, 1976.
(5) Brochard, F.; de Gennes, P. G. *Macromolecules* **1977**, *10*, 1157.
(6) Adam, M.; Delsanti, M. *Macromolecules* **1985**, *18*, 1760.
(7) Doi, M.; Onuki, A. *J. Phys. II* **1992**, *2*, 1631.
(8) Brown, W.; Štěpánek, P. In *Physical Gels*; Ross-Murphy, S., Ed.; Elsevier: New York, 1990; Chapter 9.
(9) Semenov, A. N. *Physica A* **1990**, *166*, 263.
(10) Daoud, M.; Cotton, J. P.; Farnoux, B.; Jannink, G.; Sarma, G.; Benoit, H.; Duplessix, R.; Picot, C.; de Gennes, P. G. *Macromolecules* **1977**, *8*, 804.
(11) King, J.; S.; Boyer, W.; Wignall, G. D.; Ullman, R. *Macromolecules* **1985**, *18*, 709.
(12) Ferry, J. D. *Viscoelastic Properties of Polymers*, 2nd ed.; John Wiley & Sons: New York, 1970.
(13) Table 13-II in ref 12 and using the relation $M_c \cong 2M_e$.
(14) Štěpánek, P.; Tuzar, Z.; Koňák, Č. *Collect. Czech. Chem. Commun.* **1987**, *52*, 1235.
(15) Jakeš, J. *Collect. Czech. Chem. Commun.* **1995**, *60*, 1781.
(16) Provencher, S. W. *Macromol. Chem.* **1979**, *180*, 201.
(17) Jakeš, J. *Czech J. Phys. B* **1988**, *38*, 1305.
(18) Provencher, S. W. In *Laser Light Scattering in Biochemistry*; Harding, S. E., Sattelle, D. B., Bloomfield, V. A., Eds.; Royal Society of Chemistry: London, 1992.
(19) Štěpánek, P.; Johnsen, R. *Collect. Czech. Chem. Commun.* **1995**, *60*, 1941.
(20) Štěpánek, P.; Lodge, T. P. *Macromolecules* **1996**, *29*, 1244.
(21) Brown, W.; Nicolai, T. In *Dynamic Light Scattering: The method and some applications*; Clarendon Press: Oxford, U.K., 1993; Chapter 6.
(22) Adam, M.; Delsanti, M. *Macromolecules* **1977**, *6*, 1229.
(23) Adam, M.; Delsanti, M. *J. Phys. (Paris)* ***1983***, *44*, 1185.
(24) Kanya, T.; Patkowski, A.; Fischer, E. W.; Seils, J.; Gläser, H.; Kaji, K. *Acta Polym.* **1994**, *45*, 137.
(25) Štěpánek, P.; Lodge, T. P. *Macromolecules* **1996**, *29*, 1244.
(26) Papadakis, C. M.; Brown, W.; Johnsen, R. M.; Posselt, D.; Almdal, K. *J. Chem. Phys.* **1996**, *104*, 1611.
(27) Brown, W.; Štěpánek, P. *Macromolecules* **1988**, *21*, 1791.
(28) Fischer, E. W. *Physica A* **1993**, *201*, 183.
(29) Heckmeier, M.; Mix, M.; Strobl, G. *Macromolecules* **1997**, *30*, 4454.
(30) Martin, J. E. *Macromolecules* **1986**, *19*, 1278.
(31) Wiltzius, P.; Haller, H. R.; Cannell, D. S.; Schaeffer, D. W. *Phys. Rev. Lett.* **1984**, *53*, 834.
(32) Oono, Y.; Baldwin, P. R.; Ohta, T. *Phys. Rev. Lett.* **1984**, *53*, 2149.
(33) Raspaud, E.; Lairez, D.; Adam, M. *Macromolecules* **1995**, *28*, 927.
(34) Fuchs, M.; Schweizer, K. S. *Macromolecules* **1997**, *30*, 5133.
(35) Brown, W.; Fundin, J. *Macromolecules* **1991**, *24*, 5171.
(36) de Gennes, P. G. *Scaling Concepts in Polymer Physics*; Cornell University Press: London, 1979.

MA970458U